ADVANCES IN FOREST FIRE RESEARCH

2022

Edited by
DOMINGOS XAVIER VIEGAS
LUÍS MÁRIO RIBEIRO

A statistical model of Fire Radiative Power released by wildfires at the global scale

Carlos C. DaCamara*[1]; José M. C. Pereira[2]; Renata Libonati[3]; Sílvia A. Nunes*[1]

[1]*Instituto Dom Luiz (IDL), Faculdade de Ciências, Universidade de Lisboa, 1749-016 Lisbon, Portugal, {cdcamara, sanunes}@fc.ul.pt*
[2]*Centro de Estudos Florestais, Instituto Superior de Agronomia, Universidade de Lisboa, 1349-017, Lisbon, Portugal {jmcpereira@isa.ulisboa.pt}*
[3]*Departamento de Meteorologia, Universidade Federal do Rio de Janeiro, 21941-916, Rio de Janeiro, RJ, Brasil {renata.libonati@igeo.ufrj.br}*

**Corresponding author*

Keywords

Global fire activity; Fire macroregimes; Fire Radiative Power; Truncated lognormal distribution with generalized Pareto tails

Abstract

Characterization of large-scale fire regimes associated to patterns of fire activity is especially relevant because they reflect the complex interplay of meteorological, landscape, and human factors. We present a statistical model with 8 parameters that adequately describes satellite derived fire radiative power (FRP) at the global scale and over large areas with given fire regimes. The statistical model combines three components, namely a truncated lognormal distribution central body with a lower and an upper tail, both consisting of Generalized Pareto (GP) distributions. The model is fitted to four samples of 1 000 000 values of $\log_{10} FRP$ randomly selected from a dataset consisting of observations by the MODIS instrument on-board Terra and Aqua satellites covering the 19-year period spanning from 4 July 2002 to 3 July 2021. The four samples are extracted from observations worldwide and from regions characterized by three fire macroregimes, respectively Wild, Tamed and Domesticated fires. For all four cases, the very high quality of the fit translates into the agreement between the cumulative distribution function and the respective empirical cumulative distribution function obtained from the sample. When going from the Domesticated fire macroregime to the Tamed and then to the Wild fire macroregimes, there is a progressive displacement towards the right of the respective probability distribution functions that indicates a progressive tendency for the occurrence of extreme events with a high release of radiative power that is associated with a decrease in human actions that translates into lower landscape fragmentation and lower fire suppression. Statistical model of FRP of the type here presented are a useful tool that allows characterizing in an economic way fire behaviour in a given region and monitor changes in time associated to climate change or to changes in landscape or in land occupation.

1. Introduction

The large spatiotemporal patterns of fire activity reflect on the one hand, the control exerted by climate on vegetation productivity and on fuel accumulation and respective moist content (Andela et al., 2019), and on the other hand, the effect of human actions that account for most ignitions in burnable ecosystems as well for the decrease in fire size due to landscape fragmentation and fire suppression (Bowman et al., 2009).

The identification and characterization of the large-scale fire regimes associated to patterns of fire activity as well as of the factors that condition the spatiotemporal variability of fire activity are especially important, not only because fires result from a complex interplay of meteorological, landscape, and human factors, but also because they are a source of greenhouse gases.

The characterization of fire regimes is performed by means of a set of parameters describing which fires occur in each place and time, and Earth Observation by means of satellites plays a crucial role because it represents the only means to get systematic information at the global scale during sufficiently long periods of time. Besides providing the location and date of hotspots, satellites allow estimating fire radiative power (FRP) that is a measure of combustion rate, and therefore of consumed biomass (Wooster et al., 2005).

The aim of this work is to show that satellite derived FRP, at the global scale and over large areas with given fire regimes, can be described by means of a universal statistical model with 8 parameters. This is a useful tool that allows characterizing in an economic way fire behavior in a given region and monitor changes in time associated to climate change or to changes in landscape or in land occupation.

2. Data and Methods

Information about FRP was obtained from NASA's Fire Information for Resource Management System (FIRMS) that provides location, date and hour, FRP estimates and confidence for hotspots detected by the Moderate Resolution Imaging Spectroradiometer (MODIS) on-board Terra and Aqua satellites. Extracted data consist of 85 412 052 estimates of FRP associated to all hotspots (identified as active vegetation fires) during the 19-year period spanning from 4 July 2002 to 3 July 2021. The starting date of the period is that when observations become available for both MODIS instruments on-board Terra and Aqua.

Following Pereira et al. (2022), global fires were stratified into three fire macroregimes that are interpreted according to climate type (Köppen classification) and to ecological patterns created by sustained interactions between ecosytems and humans (anthromes) (Figure 1). The three regimes (each one subdivided into a prototypical and a transitional regime) are as follows; the Wild fire macroregime predominates in cold wildlands, and is characterized by sporadic burning and short fire seasons; the Tamed fire macroregime mostly occurs in rangeland and croplands of dry tropical climate and is characterized by high fire incidence; and the Domesticated fire macroregime that is characteristic of croplands and villages in humid, warm temperate and tropical climates and is characterized by low fire incidence. Results from the stratification into the three fire macroregimes were 67 324 278 Tamed fires, 9 768 127 Domesticated fires, and 8 319 647 Wild fires, respectively representing 79%, 11% and 10% of the active fires observed worldwide.

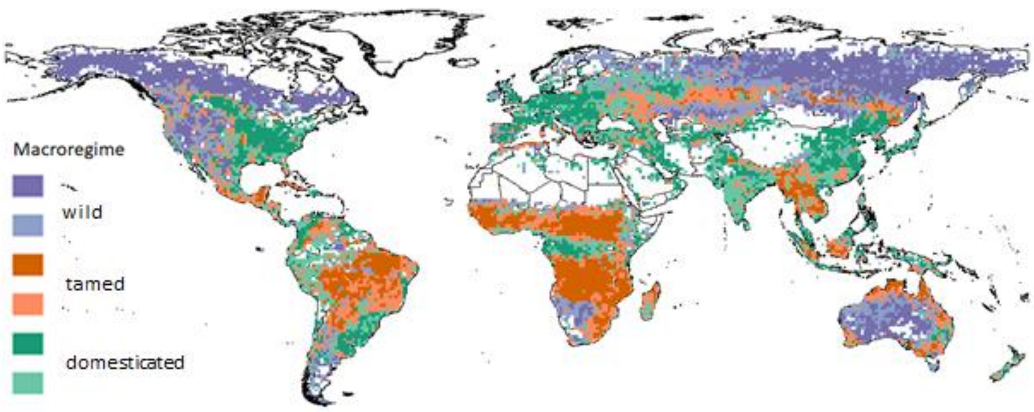

Figure 1- Global distribution of fire macroregimes; wild (violet), tamed (orange) and domesticated (green). For each macroregime, dark and light colors identify subdivision into prototypical and transitional regimes. The map was generated using information from Pereira et al. (2022).

Statistical models used in this study combine three components, namely a truncated lognormal distribution central body, f_b, with a lower and an upper tail, both consisting of Generalized Pareto (GP) distributions, f_l and f_u, respectively. The probability density function (pdf), h, for a generic random variable x is accordingly of the form:

$$h(x;\kappa_l,\sigma_l,x_l,\mu,\sigma_b,\kappa_u,\sigma_u,x_u) = \begin{cases} cbf_l(x;\kappa_l,\sigma_l,x_l), & x < x_l \\ bf_b(x;\mu_b,\sigma_b), & x_l \le x \le x_u \\ abf_u(x;\kappa_u,\sigma_u,x_u), & x > x_u \end{cases} \quad (1)$$

The lower tail GP distribution is:

$$f_l(x;\kappa_l,\sigma_l,x_l) = (1/\sigma_l)[1 + \kappa_l\,(x_l - x)/\sigma_l]^{-1-1/\kappa_l}$$

where κ_l and σ_l denote the shape and the scale parameters of f_l, and where x_l is the transition point from the lower tail GP distribution to the truncated lognormal distribution body. When $\kappa_l < 0$, the distribution has a bounded support, $x_{min} < x < x_l$, with $x_{min} = x_l + \sigma_l/\kappa_l$.

The upper tail GP distribution is:

$$f_u(x; \kappa_u, \sigma_u, x_u) = (1/\sigma_u)[1 + \kappa_u\,(x - x_u)/\sigma_u]^{-1-1/\kappa_u}$$

where κ_u and σ_u denote the shape and the scale parameters of f_u, and where x_u is the transition point from the lognormal distribution body to the upper tail GP distribution. When $\kappa_u < 0$, the distribution has a bounded support, $x_u < x < x_{max}$, with $x_{max} = x_u - \sigma_u/\kappa_u$.

Finally, the lognormal distribution central body is:

$$f_b(x; \mu_b, \sigma_b, x_l, x_u) = \exp\left[-\frac{(\ln x - \mu)^2}{2\,(\sigma_b)^2}\right] \Big/ \left[\sqrt{2\pi}\, x\, \sigma\, C(\mu, \sigma_b, x_l, x_u)\right]$$

with

$$C(\mu_b, \sigma_b, x_l, x_u) = \frac{1}{2}\left[\operatorname{erf}\left(\frac{\ln x_u - \mu_b}{\sqrt{2}\,\sigma_b}\right) - \operatorname{erf}\left(\frac{\ln x_l - \mu_b}{\sqrt{2}\,\sigma_b}\right)\right]$$

and where μ_b and σ_b are the location and scale parameters of f_b.

Normalization constants a, b, and c in equation (1) must verify the relation:

$$cb + b + ab = 1 \Rightarrow b = (a + c + 1)^{-1}$$

On the other hand, continuity of h at $x = x_l$ and at $x = x_u$ implies that:

$$cbf_l(x_l) = bf_b(x_l) \Rightarrow c = \sigma_l f_b(x_l)$$
$$abf_u(x_u) = bf_b(x_u) \Rightarrow a = \sigma_u f_u(x_u)$$

The eight parameters $(\kappa_l, \sigma_l, x_l, \mu_b, \sigma_b, \kappa_u, \sigma_u, x_u)$ of h in equation (1) are obtained by maximizing the joint log-likelihood of an i.i.d. sample of x. The rationale for the procedure consists of three steps; 1) sample values of $\ln x$ are plotted against a theoretical lognormal distribution, and first guesses of x_l and x_u are obtained by identifying the lower and upper values of x that roughly delimit the inner domain of h, where points closely form a straight line, therefore following a lognormal distribution (Chambers et al., 2017); 2) first guesses of pairs (κ_l, σ_l), (μ_b, σ_b) and (κ_u, σ_u) are then obtained using the maximum likelihood method to fit, respectively, a GP distribution to sampled values $x < x_l$, a truncated lognormal distribution to sampled values $x_l \le x \le x_u$, and a GP distribution to sampled values $x > x_u$; 3) finally, first guesses obtained in the previous two steps are used to obtain maximum likelihood estimates of the eight parameters of h.

3. Results and discussion

Since the total number of recorded events is very large (85 412 052 hot spots), a sample of 1 000 000 events was randomly selected, and the statistical model was fitted to the logarithm of FRP (i.e., $x = \log_{10} FRP$) of selected events following the procedure described in the preceding section. Results obtained are presented in Figure 2, and the very high quality of the fit is worth being emphasized; the cumulative distribution function (cdf) virtually coincides with the empirical cumulative distribution function (ecdf) obtained from the sample (Figure 2, left panel) and the probability distribution function (pdf) closely follows the histogram obtained from the sample (Figure 2, right panel).

The same procedure was applied to the recorded events belonging to the three fire macroregimes. Results obtained are presented in Figure 3, and again the very high quality of the fit for each macroregime translates into the agreement between the cdf and the respective ecdf (Figure 3, left panel). It is worth noting that when going from the Domesticated fire macroregime to the Tamed and then to the Wild fire macroregimes, there is a progressive displacement towards the right of the respective pdfs that indicates a progressive tendency for the occurrence of extreme events with a high release of radiative power that is associated with a decrease in human actions that translates into lower landscape fragmentation and lower fire suppression.

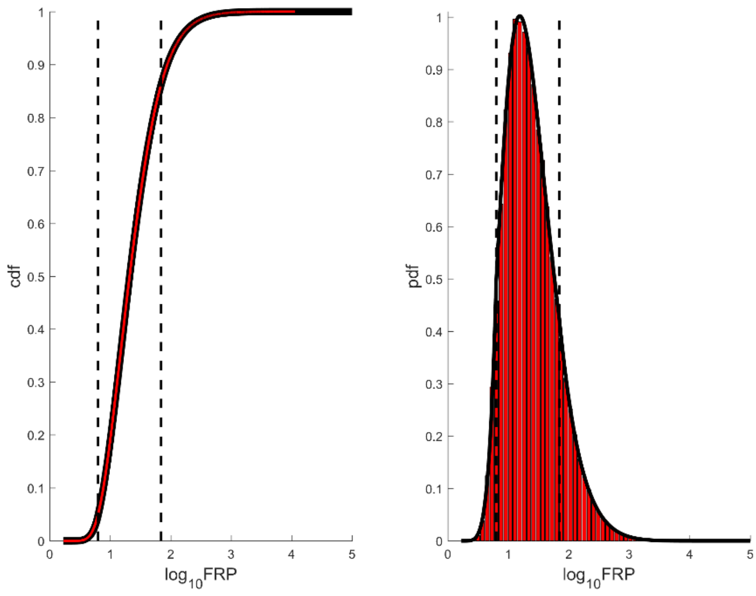

Figure 2 – Distribution of log_{10} FRP as obtained from the randomly selected sample of 1 000 000 hotspots observed worldwide during the period 04/07/2002 – 03/07/2021. Left panel: cumulated distribution function (cdf) of the fitted model (thick black curve) and empirical cumulative distribution function (ecdf) as obtained from the sample (thin red curve); right panel: probability density function (pdf) of the fitted model (thick black curve) and histogram obtained from the sample (red bars)). The two vertical dashed lines delimit the central body of the distribution.

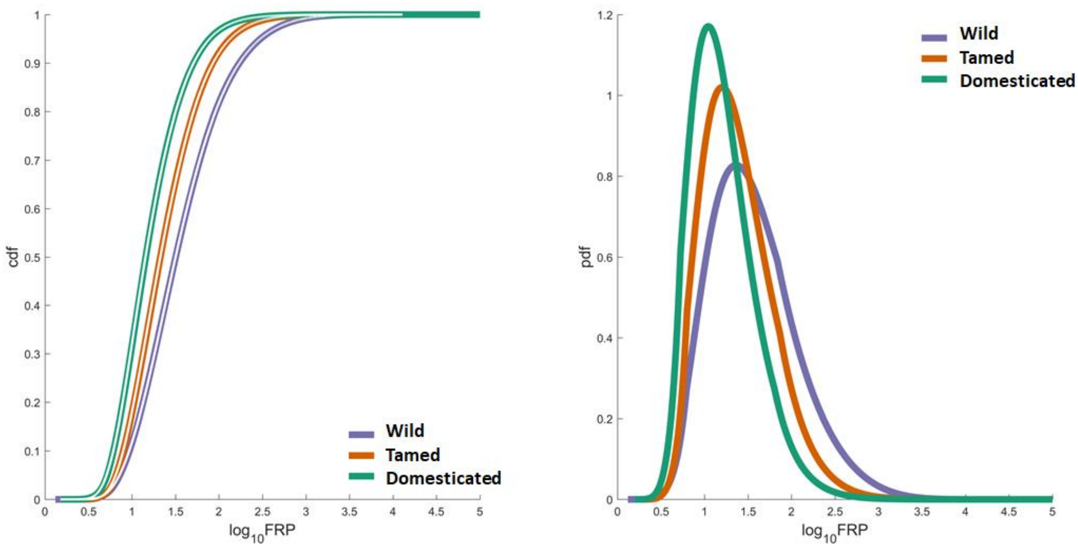

Figure 3 – Distribution of log_{10} FRP as obtained from the randomly selected sample of 1 000 000 hotspots for the Wild (violet), Tamed (orange) and Domesticated fire macroregimes during the period 04/07/2002 – 03/07/2021. Left panel: cumulated distribution function (cdf) of the fitted model (thick colored curves) and empirical cumulative distribution function (ecdf) as obtained from the sample (thin white curves); right panel: probability density function (pdf) of the fitted models.

4. Conclusion

Based on a 19-year record of satellite observations, we showed that the logarithm of FRP released by vegetation fires at the global scale closely follows a two generalized Pareto tail lognormal body distribution. The model showed to be especially useful to characterize fire macroregimes defined according to climate type and ecological patterns created by sustained interactions. Besides condensing information to a reduced number of parameters, models such as those proposed in this study allow comparing fire behavior for different periods and identifying changes in the distribution. Model of this type can be also used to calibrate meteorological indices of fire danger (DaCamara, 2014; Pinto et al. 2018) that provide operational support to decision makers on fire prevention and firefighting of rural and forest fires (DaCamara et al., 2018).

5. Acknowledgents

This work was supported by national funds through FCT (Fundação para a Ciência e a Tecnologia, Portugal) under project FIRECAST (PCIF/GRF/0204/2017), IDL (UIDB/50019/2020) and by EUMETSAT Satellite Application Facility on Land Surface Analysis (LSA SAF).

6. References

Andela, N., D. C. Morton, L. Giglio, R. Paugam, Y. Chen, S. Hantson, G. R. van der Werf, J. T. Randerson, 2019: The Global Fire Atlas of individual fire size, duration, speed and direction, Earth Syst. Sci. Data, 11, 529–552, doi:10.5194/essd-11-529-2019.

Bowman, D. M. J. S., J. K. Balch, P. Artaxo, W. J. Bond, J. M. Carlson, M. A. Cochrane, C. M. D'Antonio, R. S. Defries, J. C. Doyle, S. P. Harrison, F. H. Johnston, J. E. Keeley, M. A. Krawchuk, C. A. Kull, J. B. Marston, M. A. Moritz, I. C. Prentice, C. I. Roos, A. C. Scott, T. W. Swetnam, G. R. van der Werf, S. J. Pyne, 2009: Fire in the Earth system, Science, 324, 481–484, doi:10.1126/science.1163886

Chambers, J. M., W. S. Cleveland, B. Kleiner, P. A. Tukey, 2017: Graphical Methods for Data Analysis, Chapman and Hall/CRC, New York, doi: https://doi.org/10.1201/9781351072304

DaCamara C. C., T. J. Calado, S. L. Ermida, I. F. Trigo, M. Amraoui, K. F. Turkman KF, 2014: Calibration of the Fire Weather Index over Mediterranean Europe based on fire activity retrieved from MSG satellite imagery, Int. J. Wildland Fire, 23(7), 945-958, doi: 10.1071/WF13157

DaCamara C. C., R. M. Trigo, M. M. Pinto, S. A. Nunes, I. F. Trigo, C. M. Gouveia, M. Rainha, 2018: CeaseFire: a website to assist fire managers in Portugal. In “Advances in Forest Fire Research 2018” (D. X. Viegas, ed.), pp. 941-949, Imprensa da Universidade de Coimbra, ISBN 978-989-26-16-506, doi: 10.14195/978-989-26-16-506_103

Pereira, J. M. C., D. Oom, P. C. Silva, A. Benali, 2022: Wild, Tamed, and Domesticated: three fire macroregimes for global pyrogeography in the Anthropocene, Ecological Applications, doi: https://doi.org/10.1002/eap.2588

Pinto M. M., C. C. DaCamara, I. F. Trigo, R. M. Trigo, K. F. Turkman, 2018: Fire danger rating over Mediterranean Europe based on fire radiative power derived from Meteosat. Nat. Hazards Earth Syst. Sci. 18, 515–529, doi:10.5194/nhess-18-515-2018

Wooster, M. J., G. Roberts, G. L. W. Perry, Y. J. Kaufman, 2005: Retrieval of biomass combustion rates and totals from fire radiative power observations: FRP derivation and calibration relationships between biomass consumption and fire radiative energy release, J. Geophys. Res., 110, D24311, doi:10.1029/2005JD006318.